

# 行政院國家科學委員會專題研究計畫 成果報告

濾速遞減分析暨擾流效應對管式薄膜管超過濾與動能消耗  
之影響

研究成果報告(精簡版)

計畫類別：個別型

計畫編號：NSC 96-2221-E-032-033-

執行期間：96年08月01日至98年01月31日

執行單位：淡江大學化學工程與材料工程學系

計畫主持人：葉和明

計畫參與人員：碩士班研究生-兼任助理：陳榴儀、蔡正修

報告附件：出席國際會議研究心得報告及發表論文

處理方式：本計畫可公開查詢

中華民國 98 年 01 月 06 日

# 滲速遞減分析暨擾流效應對管式薄膜管超過濾與動能消耗之影響

葉和明

淡江大學 化學工程與材料工程學系

## **Abstract**

The correlation equations for predicting local permeate fluxes in tubular-membrane ultrafilters was derived from mass and momentum balances by the modified resistance-in-series model with the considerations of the increment of concentration polarization and the declines of transmembrane pressure and flow rate, along the membrane tube. Ultrafiltration of dextran T500 aqueous solution in a tubular microporous ceramic module has been carried out under various feed concentrations, transmembrane pressures and feed flow rates, and many experimental data of ten-point local permeate fluxes along the tube were obtained to confirm the correlation predictions. The increment of concentration polarization, as well as the decline of permeate flux, along the tube was also discussed.

*Keywords:* Ultrafiltration ; Membrane tube ; Permeate flux ; Concentration polarization

---

\*Corresponding author. Tel.: +886-2-2621-5656/ext.2601; fax: +886-2-26209887

*E-mail address:* hmyeh@mail.tku.edu.tw (H. M. Yeh)

## **1. Introduction**

Ultrafiltration membrane process has now become an increasingly important industrial process for the concentration, purification, or dewatering of macromolecular and colloidal species in solution; it is usually used in the food, beverage, and dairy industries, for effluent treatment, and biotechnology and medical applications [1-3].

The advantage of ultrafiltration as compared to conventional dewatering processes, such as evaporation, freeze concentration or freeze drying, is the absence of a change in phase or state of the solvent during dewatering process, resulting in considerable savings in energy.

Ultrafiltration is primarily a size-exclusion-based, pressure-driven membrane separation process; the pressure applied to the working fluid provides the potential to force the solvent to flow through the membrane. During operation, solute is transported to the membrane surface by the convective flow of the permeant; this is balanced by diffusion back to the bulk. In cross-flow ultrafiltration the permeate flux generally declines along the flow direction due to the phenomenon of concentration polarization by the rejected particles, which is a common feature of all pressure-driven membrane processes [4]. Several hydraulic approaches developed for reducing the effect of concentration polarization to enhance the permeate flux,

has been discussed thoroughly [5-17]. The use of inserts, such as metal grills [7], static rods [8] , spiral wire [9], disc, and doughnut shape inserts [10] and helical baffles [11-13], in a tubular membrane have been tried to different membrane processes. Da Costa and coworkers performed an extensive study of ultrafiltration flux by net-type spacers [14-17]. The applications of inserting solid and wired rods in the tubular membrane systems were also reported [5, 6]. In this study, we ultrafiltered macromolecular solution in a tubular membrane module and measured the permeate fluxes along the tube under various operating conditions. The declines of permeate flux was also analyzed by mass and momentum balances coupled with the use the modified resistance-in-series model.

## **2. Theory**

### *2.1. Resistance-in-series model*

Membrane ultrafiltration of macromolecular solutions is usually analyzed by the resistance-in-series model [5, 6], in which permeate flux decreases due to the resistances caused by fouling or solute adsorption and concentration polarization.

Although the osmotic pressure at the membrane surface also affects the permeate flux, ultrafiltration usually deals with the separation of fairly large molecules and the osmotic pressures involved in ultrafiltration processes are fairly low and negligible. According to above description of ultrafiltration in the resistance-in-series model, permeate flux  $J(z)$  may be expressed as

$$J(z) = \frac{\Delta P(z)}{R_m + R_f + R_p} \quad (1)$$

where  $R_m$  denotes the intrinsic resistance, and  $R_p$  and  $R_f$  are the resistances due to the concentration/gel layer and those due to other fouling phenomena such as adsorption, respectively, while  $\Delta P(z)$  is the transmembrane pressure defined as

$$\Delta P(z) = P(z) - P_s \quad (2)$$

In above equation,  $P(z)$  is the pressure distribution of the tube side along the axial direction  $z$ , and  $P_s$  is the permeate pressure of the shell side which may be assumed to be constant.

As mentioned before, concentration polarization is a common feature of all pressure-driven membrane processes. It is dependent on operating parameter such as pressure, temperature, feed concentration and velocity, and increases along the membrane tube. Accordingly, we may assume that for constant operating temperature

$$R_p = \beta(z) \Delta P(z) \quad (3)$$

where the proportional factor  $\beta(z)$  may be simply assumed to be linearly increasing along the tube, i.e.

$$\beta(z) = \beta_i [1 + \alpha(z/L)] \quad (4)$$

and  $\beta_i$  is the value of  $\beta$  at the inlet and  $\alpha$  is a constant ; both are to be determined experimentally . Thus, Eq. (3) may be rewritten as

$$R_p = \beta_i [1 + \alpha(z/L)] \Delta P(z) \quad (5)$$

Substitution of Eq. (5) into Eq. (1) yields

$$J(z) = \frac{\Delta P(z)}{R_m + R_f + \beta_i [1 + \alpha(z/L)] \Delta P(z)} \quad (6)$$

## 2.2. Mass balance

Figure 1 shows a microporous membrane tube of radius  $r_m$  and length  $L$  installed in the experimental apparatus. Let  $Q(z)$  be the volume flow rate of feed solution in a microporous membrane tube, a mass balance over a slice of  $dz$  of the tube gives

$$\frac{dQ}{dz} = -2\pi r_m J(z) \quad (7)$$

Integrating Eq. (7) from the inlet ( $z=0$ ,  $Q=Q_i$ ) to the outlet ( $z=L$ ,  $Q=Q_o$ ) of the tube, one has

$$Q_o = Q_i - 2\pi r_m L \bar{J} \quad (8)$$

where  $\bar{J}$  is the average value of  $J(z)$  defined as

$$\bar{J} = \frac{1}{L} \int_0^L J(z) dz \quad (9)$$

### 2.3. Momentum balance

Since the permeation rate of membrane ultrafiltration is very small compared with the volume flow rate in a membrane tube, it can be assumed that the local decline in hydraulic pressure within the membrane tube is simply given by the Hagen-Poiseuille equation in term of average volume flow rate  $\bar{Q}$  [10]

$$\frac{dP}{dz} = -\frac{8\mu\bar{Q}}{\pi r_m^4} \quad (10)$$

where

$$\bar{Q} = \frac{Q_i + Q_o}{2} = Q_i - \pi r_m L \bar{J} \quad (11)$$

Integration of Eq. (10) with the use of boundary condition:  $P = P_i$  at  $z = 0$ , results in

$$P(\xi) = P_i - \left( \frac{8\mu\bar{Q}L}{\pi r_m^4} \right) \xi \quad (12)$$

where

$$\xi = \frac{z}{L} \quad (13)$$

and the transmembrane pressure is obtained by substituting Eqs. (11) and (12) into Eq.

(2). The result is

$$\Delta P(\xi) = \Delta P_i - (mQ_i - n\bar{J})\xi \quad (14)$$

where

$$\Delta P_i = P_i - P_s \quad (15)$$

$$m = \frac{8\mu L}{\pi r_m^4} \quad (16)$$

$$n = \frac{8\mu L^2}{r_m^3} \quad (17)$$

and the transmembrane pressure at the outlet of a membrane tube is

$$\Delta P_o = \Delta P_i - (mQ_i - n\bar{J}) \quad (18)$$

#### 2.4. Permeate flux

Substitution of Eq. (14) into Eq. (6) yields the expression for local permeate flux

in a microporous membrane tube

$$J(\xi) = \frac{\Delta P_i - (mQ_i - n\bar{J})\xi}{R_m + R_f + \beta_1(1 + \alpha\xi)[\Delta P_i - (mQ_i - n\bar{J})\xi]} \quad (19)$$

The average permeate flux can be obtained by substituting Eq. (19) into Eq. (9)

$$\bar{J} = \int_0^1 J(\xi) d\xi \quad (20)$$

$$= \int_0^1 \frac{-\Delta P_i d\xi}{A\xi^2 + B\xi + C} + \int_0^1 \frac{(mQ_i - n\bar{J})\xi d\xi}{A\xi^2 + B\xi + C} \quad (21)$$

where

$$A = (mQ_i - n\bar{J})\beta_1\alpha \quad (22)$$

$$B = [(mQ_i - n\bar{J}) - \alpha\Delta P_i]\beta_1 \quad (23)$$



$$C = -(R_m + R_f + \beta_i \Delta P_i) \quad (24)$$

After integration, Eq. (21) becomes

$$\begin{aligned} \bar{J} &= \int_0^1 \frac{-\Delta P_i d\xi}{A\xi^2 + B\xi + C} + \left[ \frac{(mQ_i - n\bar{J})}{2A} \ln \left| \frac{A+B+C}{C} \right| - \frac{(mQ_i - n\bar{J})B}{2A} \int_0^1 \frac{d\xi}{A\xi^2 + B\xi + C} \right] \\ &= - \left[ \Delta P_i + \frac{(mQ_i - n\bar{J})B}{2A} \right] \int_0^1 \frac{d\xi}{A\xi^2 + B\xi + C} + \frac{(mQ_i - n\bar{J})}{2A} \ln \left| \frac{A+B+C}{C} \right| \end{aligned} \quad (25)$$

where

$$\begin{aligned} &\int_0^1 \frac{d\xi}{A\xi^2 + B\xi + C} \\ &= \frac{1}{\sqrt{B^2 - 4AC}} \ln \left| \frac{(2A+B-\sqrt{B^2-4AC})(B+\sqrt{B^2-4AC})}{(2A+B+\sqrt{B^2-4AC})(B-\sqrt{B^2-4AC})} \right|, \text{ if } B^2 > 4AC \end{aligned} \quad (26)$$

$$= \frac{2}{\sqrt{4AC - B^2}} \left[ \tan^{-1} \frac{2A+B}{\sqrt{4AC - B^2}} - \tan^{-1} \frac{B}{\sqrt{4AC - B^2}} \right], \text{ if } B^2 < 4AC \quad (27)$$

### 3. Experimental

#### 3.1. Apparatus and materials

The experimental apparatus used in this work is shown in Fig. 1. The membrane medium used was mainly 40 kDa MWCO tubular ceramic membrane (Carbsep, length  $L = 0.4$  m, inside diameter  $2r_m = 6 \times 10^{-3}$  m). The tested solute was dextran T500 (Pharmacia Co.). The solvent was distilled water. The feed solution was circulated

by a high-pressure pump with a variable feed motor (L-07553-20, Cole-Parmer Co.), the liquid flow rate was observed by a flowmeter (IR-OPFLOW 502-111, Headland Co.). The feed pressure was controlled by using an adjusting valve at the outlet of the tubular-membrane module, and the gauge pressures at the tubular inlet ( $P_i$ ), outlet ( $P_o$ ) and at shell side ( $P_p$ ) were measured with pressure transmitters (Model 891, 14, 425, Wika Co.). There were ten outlets on the shell side along the flow direction for measuring the local permeate fluxes at  $z = 2, 6, 10, 14, 18, 22, 26, 30, 34$  and  $38$  cm.

### *3.2. Experimental conditions and procedures*

The experimental conditions were as follows:

Feed concentration  $C_i$ : 0.1, 0.5, 1.0 wt%; Feed flow rate  $Q_i \times 10^6 = 1.67, 2.50, 3.33, 4.17$  m<sup>3</sup>/s;  $u_i = Q_i / \pi r_m^2 = 0.059, 0.08, 0.118, 0.147$  m/s; Feed transmembrane pressure  $\Delta P_i$ : 30, 50, 80, 110, 140 kPa.

The feed solution temperature in all experiments was kept at 25°C by a thermostat. During a run both the permeate and the retentate were recycled back to the feed tank. The experimental procedure was as follows. First, a fresh tubular-membrane module was used to measure the permeate fluxes of pure-water

ultrafiltration  $J_w$ , for determining the intrinsic resistance of the membrane. Next, the steady permeate fluxes of liquid solution at the ten outlets,  $z_j = [2+4(j-1)] \times 10^{-2}$  m,  $j = 1 \sim 10$ , were measured under various  $C_i$ ,  $Q_i$ , and  $\Delta P_i$ . After each experimental run, the membrane was cleaned by the methods of high circulation and backflushing with 10% NaOH solution, 10% HNO<sub>3</sub> solution and water. The cleaning procedure was repeated until the original water flux has been restored. Many experimental data were obtained and some of them are listed in Tables 1-5.

### 3.3. Determination of $R_m$ and $R_f$

The experimental data of the average permeate fluxes for pure water  $(\bar{J}_w)_{\text{exp}}$  and solution  $(\bar{J})_{\text{exp}}$  are presented in Tables 1 and 2, respectively. With the use of Table 1, a straight line of  $(1/\bar{J}_w)_{\text{exp}}$  versus  $(1/\Delta P)_{\text{exp}}$  could be constructed by the least-square method. Thus, the intrinsic resistance of the membrane tube employed in this study can be determined from Table 1 by using the following equation which can be modified from Eq. (1) by setting  $R_f = 0$  and  $R_p = 0$  for pure-water ultrafiltration

$$\frac{1}{(\bar{J}_w)_{\text{exp}}} = \frac{R_m}{(\Delta P)_{\text{exp}}} \quad (28)$$

In above equation the average transmembrane pressure may be estimated by taking

the arithmetic mean, according to the linear function of Eq. (12) as

$$\left(\overline{\Delta P}\right)_{\text{exp}} = \frac{1}{2} \left[ \left(\Delta P_i\right)_{\text{exp}} + \left(\Delta P_o\right)_{\text{exp}} \right] \quad (29)$$

in which  $\left(\Delta P_i\right)_{\text{exp}}$  and  $\left(\Delta P_o\right)_{\text{exp}}$  are the experimental values of inlet and outlet transmembrane pressures. Under various  $Q_i$  and  $\left(\overline{\Delta P}\right)_{\text{exp}}$ , the measured value of  $R_m$

for the membrane system employed in present study was determined graphically in

Fig.2 as

$$R_m = 1.0492 \times 10^{10} \text{ Pa} \cdot \text{s/m} \quad (30)$$

Furthermore, the experimental data obtained in ultrafiltration of an aqueous solution may be also applied to determine  $R_f$  by Eq.(1) coupled with the use of Eq.(3) [ 8 , 9 ] as

$$\left(\overline{J}\right)_{\text{exp}} = \frac{\left(\overline{\Delta P}\right)_{\text{exp}}}{R_m + R_f + \beta \left(\overline{\Delta P}\right)_{\text{exp}}} \approx \frac{\left(\overline{\Delta P}\right)_{\text{exp}}}{R_m + R_f + \phi \left(\overline{\Delta P}\right)_{\text{exp}}}$$

or

$$\frac{1}{\left(\overline{J}\right)_{\text{exp}}} = \phi + \frac{R_m + R_f}{\left(\overline{\Delta P}\right)_{\text{exp}}} \quad (31)$$

Therefore, from a straight line plot of  $(1/\overline{J})_{\text{exp}}$  versus  $(1/\overline{\Delta P})_{\text{exp}}$ , similar to Fig.2 ,

with the use of Table 2 , the values of  $\phi$  (the intersection at the ordinate) and  $(R_m+R_f)$

(the slope), as well as  $R_f$ , were determined graphically . The results are given in Table

3 for various  $u_i$  ( =  $Q_i / \pi r_m^2$  ) and  $C_i$ . Finally , the following correlation equations

for  $\phi$  and  $R_f$  were constructed as

$$\phi = 1.426 \times 10^5 u_i^{-0.39} C_i^{0.56} \quad (32)$$

$$R_f = 1.075 \times 10^9 u_i^{-0.73} C_i^{0.44} \quad (33)$$

#### 3.4. Determination of $\beta_i$ and $\alpha$

Again, if the experimental data for the local permeate flux ,  $J(z)$  , in Tables 4 and 5 and transmembrane pressure ,  $\Delta P(z)$ , are applied to Eq. (1) coupled with the use of Eq.(3) ,  $R_p = \beta(z)\Delta P(z)$ , then

$$\beta(z) = \frac{1}{[J(z)]_{\text{exp}}} - \frac{R_m + R_f}{[\Delta P(z)]_{\text{exp}}} \quad (34)$$

where, according to the linear decline of transmembrane pressure shown in Eq. (14)

$$[\Delta P(z)]_{\text{exp}} = (\Delta P_i)_{\text{exp}} - [(\Delta P_i)_{\text{exp}} - (\Delta P_o)_{\text{exp}}](z/L) \quad (35)$$

Some values of  $\beta(z)$  obtained from Eq. (34) with known values of  $(R_m+R_f)$ ,  $[J(z)]_{\text{exp}}$  and  $[\Delta P(z)]_{\text{exp}}$ , are also listed in Tables 4 and 5. Therefore, from a straight-line plot of  $\beta(\xi)$  versus  $\xi$  at a certain flow velocity  $u_i$  and feed concentration  $C_i$ , as shown in Fig. 3, the experimental values of  $\beta_i$  (the intersection at the ordinate) and  $\beta_i\alpha$  (the slope) were determined graphically, according to Eq. (4). Finally, the correlation equations for  $\beta_i$  and  $\alpha$  were constructed as

$$\beta_i = 3.54 \times 10^5 u_i^{-0.021} C_i^{0.373} \quad (36)$$

$$\alpha = 2.43 \times 10^{-3} u_i^{-1.666} C_i^{0.592} \quad (37)$$

## 4. Results and discussion

### 4.1. Comparison of correlation predictions with experimental results

The average values of permeate flux  $\bar{J}$  may be predicted from Eqs. (25)-(27) by trial-and-error method coupled with the use of the correlation equations, Eqs. (30), (33), (36) and (37), and the system constants:  $L= 0.4$  m,  $r_m = 0.03$  m, and the fluid viscosity [8]:

$$\mu = 0.894 \times 10^{-3} \exp(0.408C_i) \quad (\text{Pa} \cdot \text{s}) \quad (38)$$

Correlation predictions for  $\bar{J}$  were thus calculated and some of the results are compared with the experimental data, as shown in Fig. 4. It is seen in this figure that the present model does not predict  $\bar{J}$  well for higher transmembrane pressure .

The local values of permeate flux  $J(\xi)$  can be also predicted if the values of  $\bar{J}$  thus obtained and above same correlation equations and system constants are substituted into Eq. (19). Some prediction results are compared with the experimental results, as shown in Figs. 5 and 6. The prediction results for local permeate fluxes obtained from the traditional resistance-in-series model [5,6] with  $\beta(\xi)$  replaced by a proportional constant,  $\phi$  , were calculated by Eq.(1) coupled with the use of Eqs.

(30) , (32) and (33) , and are also plotted in these figures. It is seen that the modified resistance-in-series model with the variable concentration-polarization resistance,  $R_p = \beta_i(1 + \alpha\xi)\Delta P(\xi)$  , is more precisely applicable than the conventional resistance-in-series model [5,6],

$$J(z) = \frac{\Delta P(z)}{R_m + R_f + \phi\Delta P(z)} \quad (39)$$

in which the term of concentration-polarization resistance,  $R_p = \phi\Delta P(\xi)$  , is nearly unchanged but slightly declined along the tube, as also shown in Figs. 7 and 8.

#### 4.2. Concentration polarization increment

The decline of permeate flux along the cross-flow direction is mainly due to the decrease of transmembrane pressure  $\Delta P(\xi)$  (driving force) and the increase of concentration polarization  $R_p(\xi)$  (resistance). Figs. 7 and 8 show the variations of  $R_p(\xi)$  along the flow direction, with the traditional model defined in previous works [5, 6],  $\phi\Delta P(\xi)$  , and with the modified model defined in present study,  $\beta_i(1 + \alpha\xi)\Delta P(\xi)$  . It is obvious that the traditional model gives the incorrect description of  $R_p(\xi)$  , decreasing, instead of increasing, along the membrane tube. The correct definition of  $R_p(\xi)$  by Eq. (5) does increase in the cross-flow direction,

and the increment turns to more sensitive as the solution concentration increases or the fluid velocity decreases. The variations of concentration polarization may be also compared directly by the following expressions :

$$[R_p(\xi)/R_p(0)]_\phi = [\Delta P(\xi)/\Delta P_i] = 1 - (mQ_i - n\bar{J})(\xi/\Delta P_i) \quad (40)$$

$$[R_p(\xi)/R_p(0)]_{\beta(\xi)} = [(1 + \alpha\xi)\Delta P(\xi)/\Delta P_i] = (1 + \alpha\xi)[R_p(\xi)/R_p(0)]_\phi \quad (41)$$

## 5. Conclusion

The correlation equations, Eqs. (19) and (25), for predicting the local and average values of the permeate flux, respectively, in tubular-membrane ultrafilters, were derived from mass and momentum balances by the modified resistance-in-series model with the considerations of the increment of concentration polarization and the declines of transmembrane pressure and flow rate, along the membrane tube. The declines of flow rate, transmembrane pressure and permeate flux along the tube may be predicted from Eqs. (7), (14) and (19), respectively. For predicting the increment of concentration polarization, one may employ Eq. (5) coupled with the use of Eq. (14). Ultrafiltration of dextran T500 aqueous solution in a tubular microporous ceramic module has been carried out under various feed concentrations, transmembrane



pressures and feed flow rates. Correlation predictions are compared with the experimental results, as shown in Figs. 4-6. It is found that the correlation predictions of local permeate flux obtained from present modified resistance-in-series model are more accurate than those obtained from the conventional resistance-in-series model [5, 6] , in which the concentration-polarization resistance was described by an incorrect term,  $\phi\Delta P(\xi)$  , decreasing slightly along the tube, while in present study, the increment of concentration polarization,  $\beta_1(1+\alpha\xi)\Delta P(\xi)$  , through the tube was taken into consideration, resulting in the correct decline of permeate flux, as confirmed by experiments. Therefore, the present model easily described the relationships of the decline of permeate flux with operating and design parameters, and we believe that this model will also suitable for most membrane ultrafiltration systems including systems with different kinds of feed solutions, different materials of membrane tubes, and various design and operating conditions.

### **Acknowledgements**

The authors wish to express their thanks to the National Science Council of ROC for financial aid with Grant No. NSC 96-2221-E-032-033 .

## Nomenclature

### *List of symbols*

A, B, C	system constant, defined by Eq. (22), Eq. (23), Eq. (24) (Pa s/m)
$C_i$	concentration of feed solution (wt% dextran T500)
J	permeate flux of solution ( $\text{m}^3/(\text{m}^2 \text{ s})$ )
L	effective length of membrane tube (m)
m, n	constant, defined by Eq. (16), Eq. (17) ( $\text{Pa s/m}^3$ )
P	pressure distribution on the tube side (Pa)
$P_s$	uniform permeate pressure on the shell side (Pa)
$\Delta P$	transmembrane pressure, $P - P_s$ (Pa)
Q	volume flow rate in a tubular-membrane module ( $\text{m}^3/\text{s}$ )
$r_m$	inside radius of membrane tube (m)
$R_f$	resistance due to solute adsorption and fouling (Pa s/m)
$R_m$	intrinsic resistance of membrane (Pa s/m)
$R_p$	resistance due to concentration polarization (Pa s/m)
u	fluid velocity in the membrane tube, $Q/(\pi r_m^2)$ (m/s)
z	axial coordinate (m)
$z_j$	$j = 1, 2, \dots, 10$ , permeate fluxes exit at these ten points (m)

### *Greek letters*

$\alpha$	constant, defined in Eq. (4)
----------	------------------------------

$\beta(z)$	linear function of $z$ , defined in Eq. (4) (s/m)
$\phi$	constant defined by Eqs. (3) and (39) (s/m)
$\mu$	viscosity of solution (Pa s)
$\xi$	dimensionless axial coordinate, $z/L$

### *Subscripts*

i	at the inlet
o	at the outlet
w	of pure water

### *Superscript*

—	average value
---	---------------

### **References**

- [1] M. C. Porter, Membrane filtration, in P. A. Schweitzer (Ed), Handbook of Separation Techniques for Chemical Engineers, McGraw-Hill, New York, 1979, Sect. 2.1.
- [2] M. Cheryan, Ultrafiltration Handbook, Technomic Publishing Co., Lancaster, PA, 1986, Sect. 8.
- [3] M. Cheryan, N. Rajagopalan, Membrane processing of oily streams: wastewater treatment and waste reduction, J. Membr. Sci. 151 (1998)13.
- [4] A. G. Fane, Ultrafiltration: factors influencing flux and rejection, in: R. J. Wakeman (Ed.), Progress in Filtration and Separation, vol. 4, Elsevier,

Amsterdam, 1986.

- [5] H. M. Yeh, H. Y. Chen, K. T. Chen, Membrane ultrafiltration in a tubular module with a steel rod inserted concentrically for improved performance, *J. Membr. Sci.* 168 (2000) 121.
- [6] H. M. Yeh, K. T. Chen, Improvement of ultrafiltration performance in tubular membranes using a twisted wire-rod assembly, *J. Membr. Sci.* 178 (2000) 43.
- [7] D.C. Thomas, Enhancement of forced convection heat transfer coefficient using detached turbulent promoters, *Ind. Eng. Chem. Process Design Dev.*, 6 (1967) 385.
- [8] C. Peri, W. L. Dunkley, Reverse osmosis of cottage cheese whey, Influence of flow conditions, *J. Food Sci.*, 36 (1971) 395.
- [9] S. Poyen, F. Quemeneur, B. Bariou, Improvement of the flux of permeate in ultrafiltration by turbulence promoters, *Int. Chem. Eng.*, 27 (1987) 441.
- [10] J. A. Howell, R. W. Field, Dengxi Wu, Yeast cell microfiltration: flux enhancement in baffled and pulsatile flow system, *J. Membr. Sci.*, 80 (1993) 59.
- [11] B. B. Gupta, D. Wu, R.W. Field, J. A. Howell, Permeate flux enhancement using a baffle in microfiltration with mineral membrane, in: E. F. Vasant (Ed.), *Separation Technology vol.11*, Elsevier Science BV, 1994, p.559.
- [12] B. B. Gupta, J. A. Howell, D. Wu, R. W. Field, A helical baffle for cross- flow microfiltration, *J. Membr. Sci.*, 99 (1995) 31.
- [13] J. A. Howell, R. W. Field, D. Wu, Ultrafiltration of high viscosity solution: theoretical developments and experimental findings, *Chem. Eng. Sci.*, 51 (1996) 1405.
- [14] A. R. Da Costa, A. G. Fane, C. J. D. Fell, A. C. M. Franker, Optimal channel

- spacer design for ultrafiltration, *J. Membr. Sci.*, 62 (1991) 275.
- [15] A. R. Da Costa, A. G. Fane, D. E. Wiley, Spacer characterization and pressure drop modeling in Spacer-filled channels for ultrafiltration, *J. Membr. Sci.*, 87 (1994) 79.
- [16] A. R. Da Costa, A. G. Fane, Net-type spacers: Effect of configuration on fluid flow path and ultrafiltration flux, *Ind. Eng. Chem. Res.*, 33 (1994) 1845.
- [17] R. W. Field, D. Wu, J. A. Howell, B. B. Gupta, Critical flux concept for microfiltration fouling, *J. Membr. Sci.*, 100 (1995) 259.
- [18] B. H. Chiang, M. Cheryan, Ultrafiltration on skin milk in hollow fibers, *J. Food Sci.* 51 (1986) 340.
- [19] H. Nabetani, M. Nakajima, A. Watanabe, S. Nakao, S. Kumura, Effects of osmotic pressure and adsorption on ultrafiltration of ovalbumin, *AIChE J.* 360 (1990)907.
- [20] M. Assadi, D. A. White, A model for determining the steady state flux of inorganic microfiltration membrane, *Chem. Eng. J.* 48 (1992) 11.

## Figure Legends

- Fig. 1 Experimental apparatus.
- Fig. 2 A straight line of  $(1/\bar{J}_w)_{\text{exp}}$  vs.  $(1/\Delta P)_{\text{exp}}$
- Fig. 3 A straight line of  $\beta$  vs.  $\xi$ .
- Fig. 4 Comparison of experimental results of  $\bar{J}$  with correlation predictions for  $C_i = 1.0$  wt%.
- Fig. 5 Comparison of experimental results of  $J(z)$  with correlation predictions for  $C_i = 0.1$  wt% and  $u_i = 0.059$  m/s.
- Fig. 6 Comparison of experimental results of  $J(z)$  with correlation predictions for  $C_i = 1.0$  wt % and  $u_i = 0.147$  m/s .
- Fig. 7 Variation of concentration polarization along the tube for  $C_i = 0.1$  wt% and  $\Delta P_i = 80$  kPa.
- Fig. 8 Variation of concentration polarization along the tube for  $C_i = 1.0$  wt% and  $\Delta P_i = 80$  kPa.

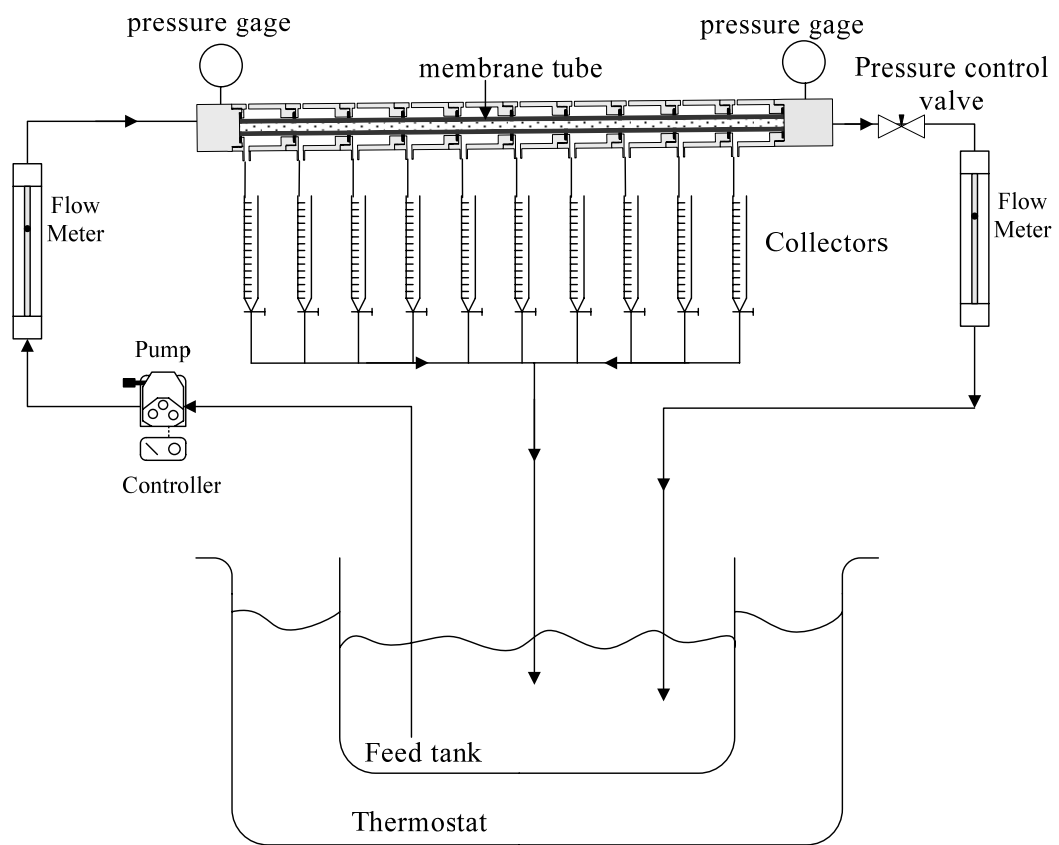


Fig. 1

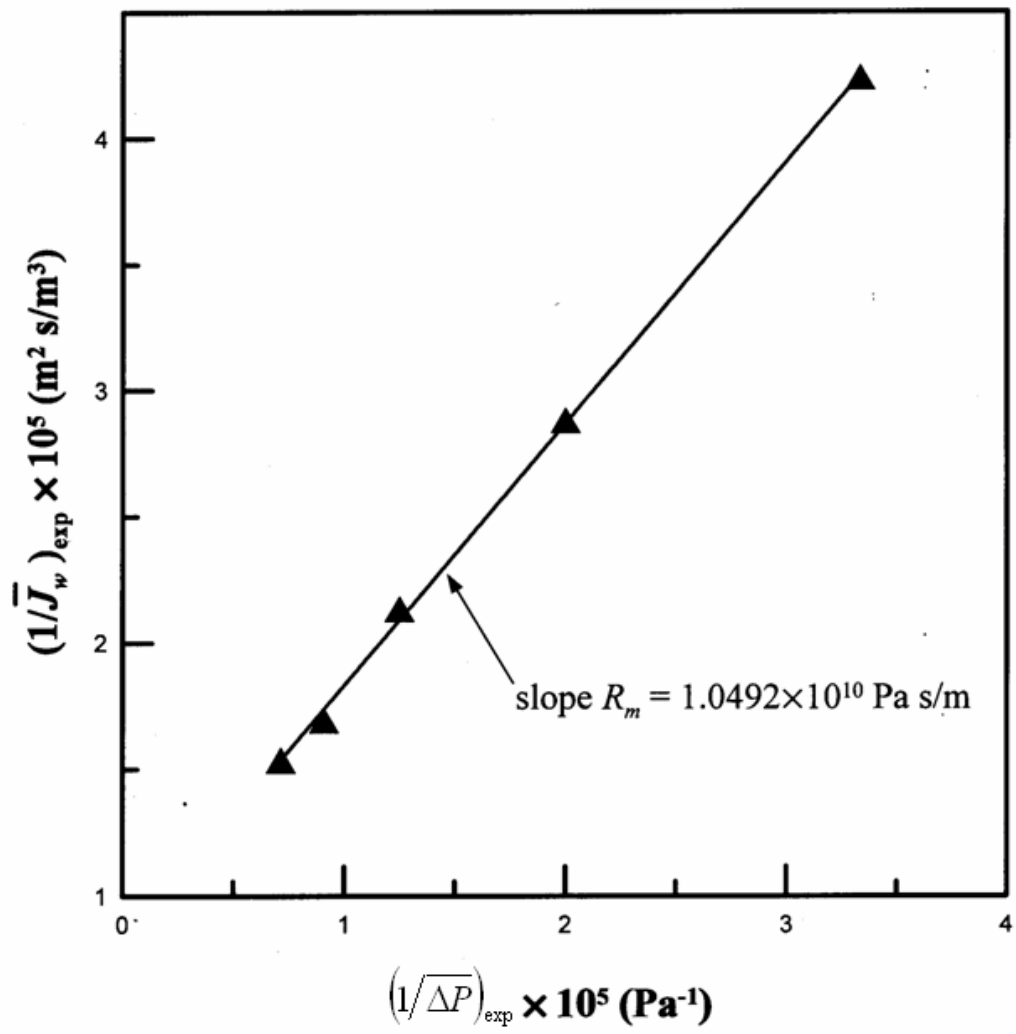


Fig. 2



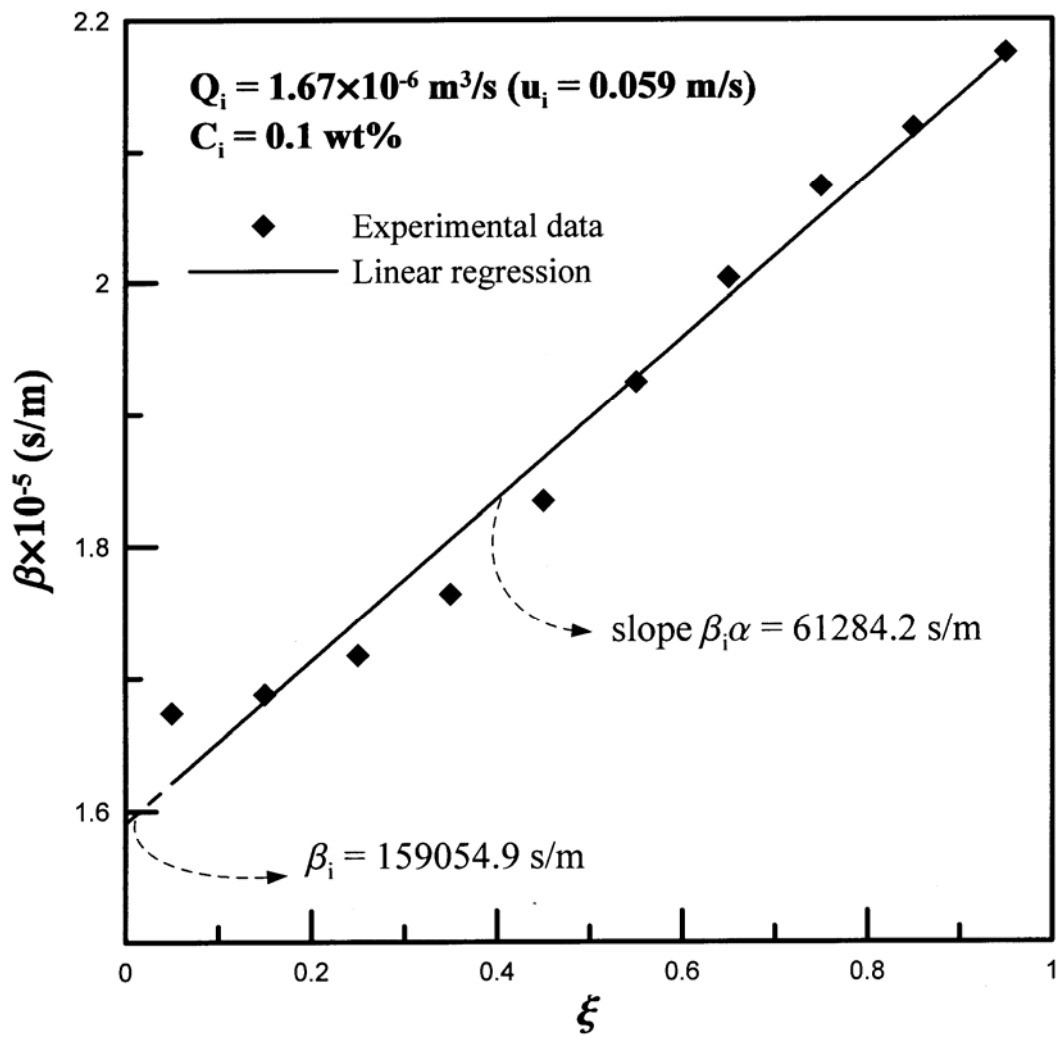


Fig. 3

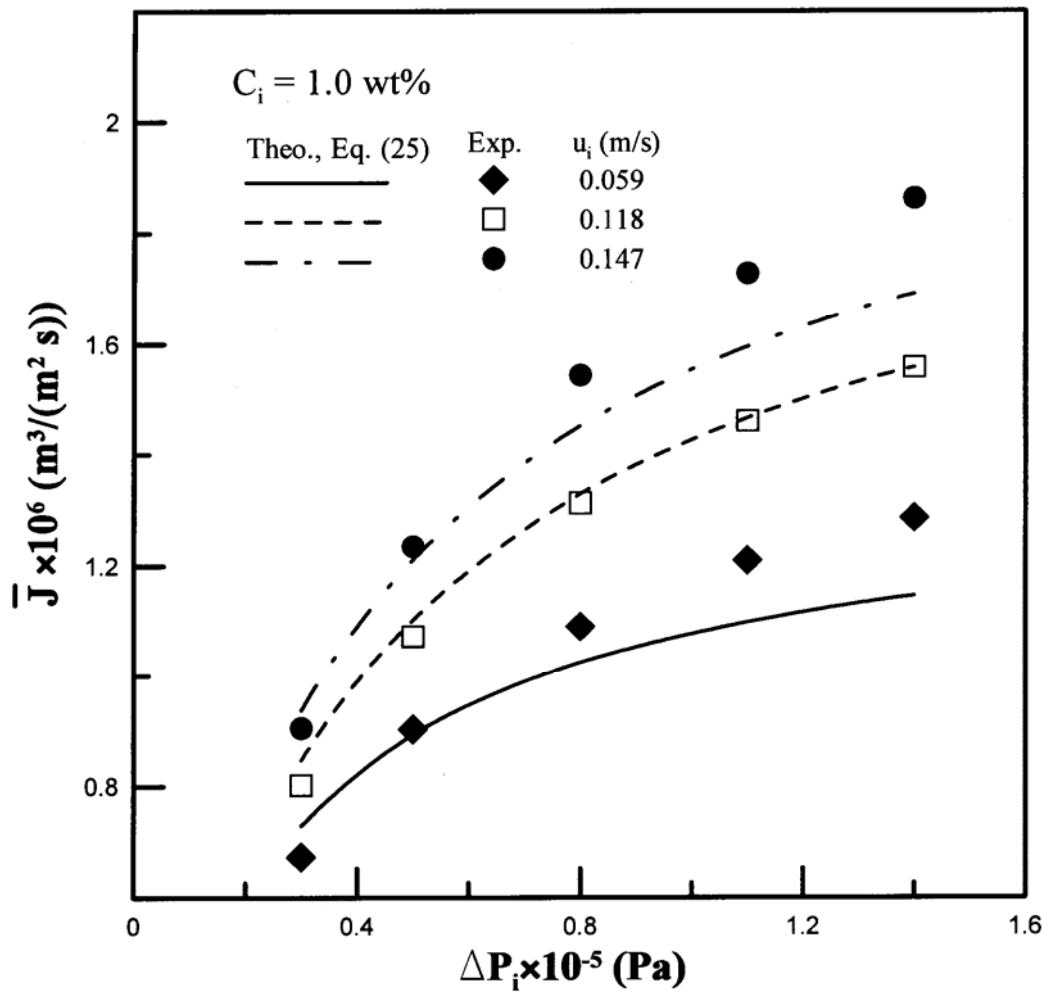


Fig. 4

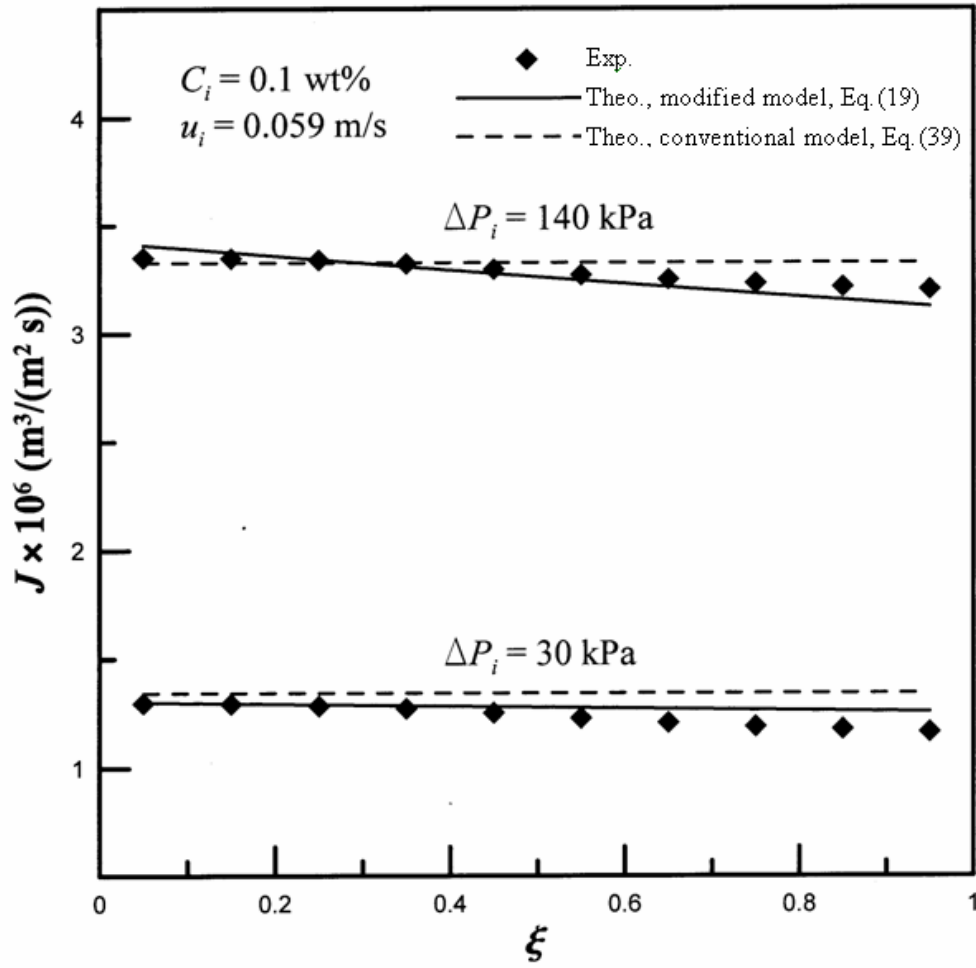


Fig . 5

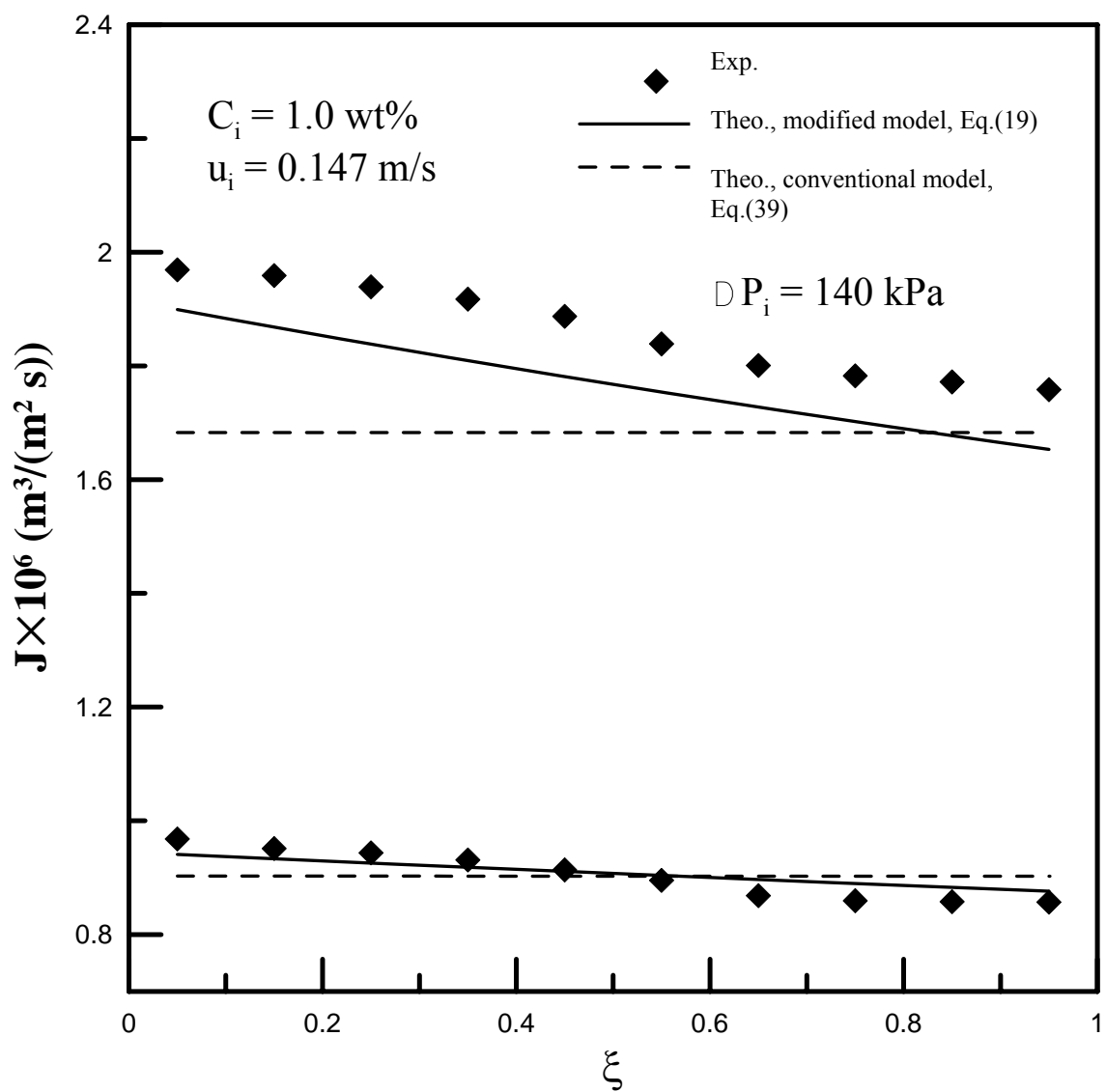
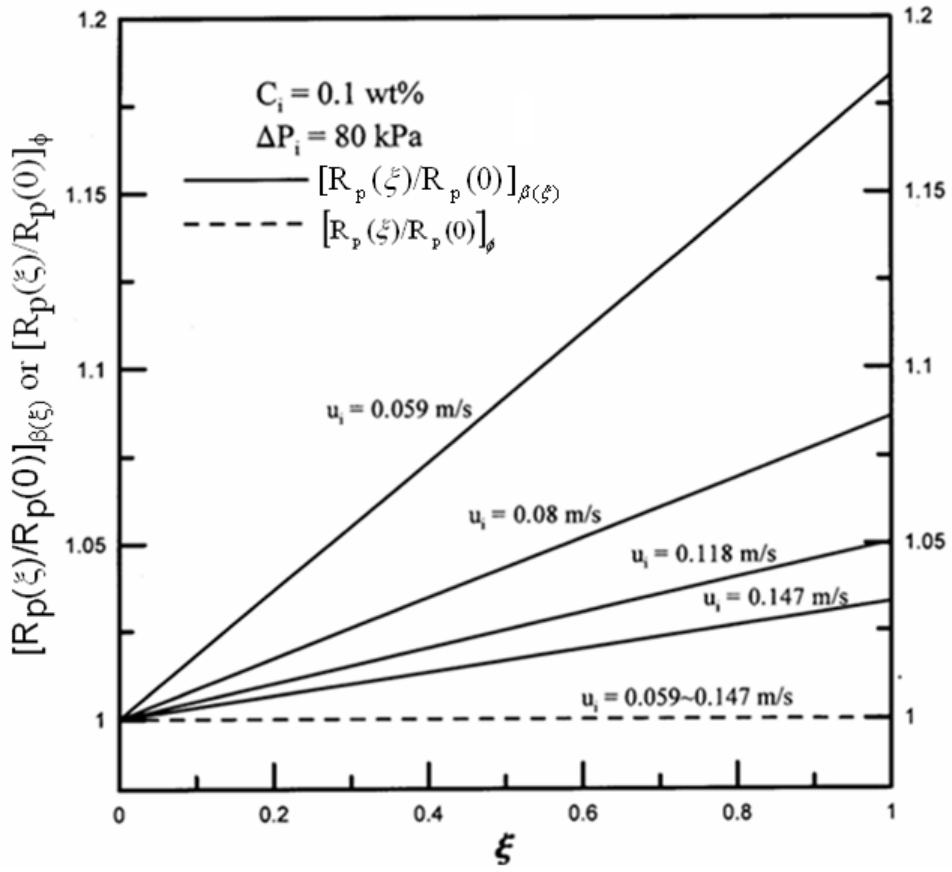


Fig . 6



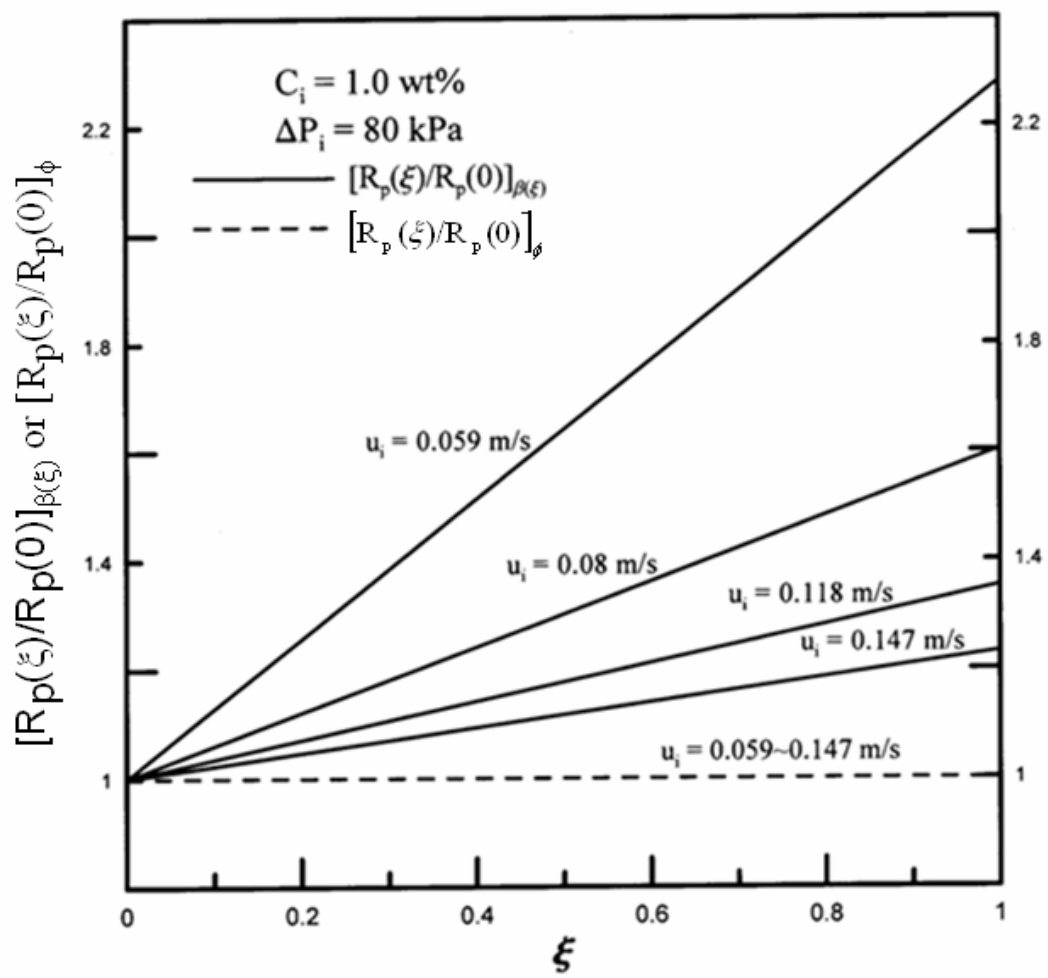


Fig. 8

**Table 1**Experimental data of permeate flux for pure water with  $u_i = 0.147$  m/s

$\Delta P_i \times 10^{-5}$ (Pa)	$\Delta P_o \times 10^{-5}$ (Pa)	$\overline{\Delta P} \times 10^{-5}$ (Pa)	$\bar{J}_w \times 10^6$ ( $\text{m}^3/(\text{m}^2 \text{ s})$ )
0.3	0.29953	0.29977	2.358
0.5	0.49953	0.49977	3.472
0.8	0.79953	0.79977	4.684
1.1	1.09953	1.09977	5.913
1.4	1.39953	1.39977	6.517

**Table 2**

Experimental data of average permeate flux for dextran T500 aqueous solution

$C_i$ (wt%)	$Q_i \times 10^6 = 1.67 \text{ m}^3/\text{s}$		$Q_i \times 10^6 = 2.50 \text{ m}^3/\text{s}$		$Q_i \times 10^6 = 3.33 \text{ m}^3/\text{s}$		$Q_i \times 10^6 = 4.17 \text{ m}^3/\text{s}$	
	$\overline{\Delta P} \times 10^{-5}$ (Pa)	$\bar{J} \times 10^6$ ( $\text{m}^3/\text{m}^2 \cdot \text{s}$ )	$\overline{\Delta P} \times 10^{-5}$ (Pa)	$\bar{J} \times 10^6$ ( $\text{m}^3/\text{m}^2 \cdot \text{s}$ )	$\overline{\Delta P} \times 10^{-5}$ (Pa)	$\bar{J} \times 10^6$ ( $\text{m}^3/\text{m}^2 \cdot \text{s}$ )	$\overline{\Delta P} \times 10^{-5}$ (Pa)	$\bar{J} \times 10^6$ ( $\text{m}^3/\text{m}^2 \cdot \text{s}$ )
0.1	0.296	1.2372	0.302	1.3972	0.303	1.5757	0.308	1.7496
	0.504	1.8288	0.507	2.0748	0.492	2.3458	0.487	2.5814
	0.805	2.4722	0.792	2.8172	0.805	3.1927	0.801	3.4792
	1.093	2.9387	1.096	3.3594	1.112	3.8139	1.109	4.1268
	1.407	3.2828	1.393	3.7646	1.403	4.2798	1.382	4.6065
0.5	0.293	0.8161	0.295	0.8654	0.283	0.9664	0.296	1.0442
	0.492	1.0959	0.493	1.1669	0.489	1.3112	0.496	1.4288
	0.814	1.3463	0.805	1.4391	0.793	1.6261	0.806	1.7858
	1.082	1.5011	1.103	1.6084	1.105	1.8238	1.093	2.0127
	1.393	1.6056	1.409	1.7216	1.386	1.9569	1.409	2.1667
1.0	0.294	0.6733	0.291	0.7195	0.288	0.8024	0.302	0.9046
	0.497	0.9027	0.498	0.9542	0.495	1.0726	0.508	1.2354
	0.793	1.0903	0.792	1.1591	0.806	1.3126	0.802	1.5436
	1.108	1.2104	1.112	1.2834	1.108	1.4602	1.098	1.7279
	1.386	1.2868	1.385	1.3654	1.417	1.5578	1.384	1.8624



**Table3**Experimental data for  $R_f$  and  $\phi$ 

$C_i$ (wt%)	$Q_i \times 10^6$ (m <sup>3</sup> /s)	$(R_m + R_f) \times 10^{-10}$ (Pa · s/m)	$R_f \times 10^{-10}$ (Pa · s/m)	$\phi \times 10^{-5}$ (s/m)
0.1	1.67	1.8154	0.7662	1.738
	2.50	1.6219	0.5727	1.489
	3.33	1.4449	0.3957	1.296
	4.17	1.2773	0.2281	1.251
0.5	1.67	2.1702	1.1210	4.668
	2.50	2.0709	1.0217	4.317
	3.33	1.8873	0.8381	3.751
	4.17	1.7878	0.7386	3.328
1.0	1.67	2.5473	1.4981	5.918
	2.50	2.3691	1.3199	5.617
	3.33	2.1779	1.1287	4.851
	4.17	2.0477	0.9985	3.893

**Table 4**

The fitting parameter of experimental data for  $C_i = 0.1$  wt% and  $Q_i = 1.67 \times 10^{-6} \text{ m}^3/\text{s}$

$z \times 1 \beta \times 10^{-5}$		$\Delta P_i = 0.3 \times 10^5 \text{ Pa}$			$\Delta P_i = 1.4 \times 10^5 \text{ Pa}$		
(m)	(s/m)	$\Delta P \times 10^{-5}$ (Pa)	$J \times 10^6$ (m/s)	$\beta \Delta P (=R_p)$ $\times 10^{-10}$ (Pa s/m)	$\Delta P \times 10^{-5}$ (Pa)	$J \times 10^6$ (m/s)	$\beta \Delta P (=R_p)$ $\times 10^{-10}$ (Pa s/m)
2	1.6736	0.2999	1.2969	0.5019	1.4000	3.3516	2.3430
6	1.6876	0.2996	1.2928	0.5056	1.3997	3.3474	2.3621
10	1.7174	0.2994	1.2841	0.5142	1.3995	3.3395	2.4035
14	1.7635	0.2991	1.2714	0.5275	1.3992	3.3233	2.4675
18	1.8342	0.2989	1.2528	0.5482	1.3990	3.2962	2.5660
22	1.9243	0.2986	1.2289	0.5746	1.3987	3.2693	2.6915
26	2.0032	0.2984	1.2082	0.5978	1.3985	3.2497	2.8015
30	2.0729	0.2981	1.1906	0.6179	1.3982	3.2319	2.8983
34	2.1181	0.2979	1.1801	0.6310	1.3980	3.2155	2.9611
38	2.1749	0.2976	1.1661	0.6473	1.3977	3.2031	3.0399

**Table 5**

The fitting parameter of experimental data for  $C_i = 1.0 \text{ wt}\%$  and  $Q_i = 4.17 \times 10^{-6} \text{ m}^3/\text{s}$

$z \times 1 \beta \times 10^{-5}$		$\Delta P_i = 0.3 \times 10^5 \text{ Pa}$			$\Delta P_i = 1.4 \times 10^5 \text{ Pa}$		
		$\Delta P \times 10^{-5}$ (Pa)	$J \times 10^6$ (m/s)	$\beta \Delta P (=R_p)$ $\times 10^{-10}$ (Pa s/m)	$\Delta P \times 10^{-5}$ (Pa)	$J \times 10^6$ (m/s)	$\beta \Delta P (=R_p)$ $\times 10^{-10}$ (Pa s/m)
2	3.5602	0.2995	0.9681	1.0663	1.3996	1.9691	4.9829
6	3.6647	0.2986	0.9513	1.0943	1.3987	1.9588	5.1258
10	3.7323	0.2977	0.9438	1.1111	1.3978	1.9391	5.2170
14	3.8335	0.2968	0.9311	1.1378	1.3969	1.9175	5.3550
18	3.9788	0.2959	0.9135	1.1773	1.3960	1.8871	5.5544
22	4.1603	0.2950	0.8952	1.2273	1.3951	1.8387	5.8040
26	4.3905	0.2941	0.8683	1.2912	1.3942	1.8008	6.1212
30	4.4770	0.2931	0.8596	1.3122	1.3932	1.7826	6.2374
34	4.5055	0.2922	0.8579	1.3165	1.3923	1.7718	6.2730
38	4.5325	0.2913	0.8571	1.3203	1.3914	1.7583	6.3065

## 出席國際學術會議心得報告

計畫編號	NSC 96-2221-E-032-033-
計畫名稱	濾速遞減分析暨擾流效應對管式薄膜管超過濾與動能消耗之影響
出國人員姓名 服務機關及職稱	葉和明、淡江大學、教授
會議時間地點	自 96 年 11 月 4 日至 96 年 11 月 9 日，美國 Utah 州鹽湖城
會議名稱	2007 年美國化工學會年會暨研討會
發表論文題目	Effect of Concentration Polarization on Flux Decline for Ultrafiltration in Tubular Membranes

### 一、參加會議經過

2007 年美國化工學會研討會於十一月四日於美國 Utah 州鹽湖城(Salt Lake City)揭幕，其中包括辦理註冊報到手續及領取資料並瞭解會場。次日即開始參與有關之研討會。本會討論化工製造及應用技術，含六百六十討論項目，由來自世界各國之專家學者共發表約六千餘篇論文，故富重要性、學術性及國際性。大會在十一月九日的結束。

### 二、與會心得

2007 年美國化工學會研討會的規模宏大，參加人數眾多。討論項目涵蓋六百六十子題，共有六千餘篇論文發表。會中除宣讀論文外，亦能有機會跟與會有關學人互相交換意見，獲益良多，可供往後研究方向及研究方法之參改，值得參加。沿途順道參觀名校「柏克萊加州大學」並收集一些有關今後的研究資料。國人研究同一領域之學者人數極為有限，因此若能經常出席國際學術研討會，可藉此宣揚，同時也可增進國民外交。因此有關此會議之參與，政府應積極鼓勵與資助。